The Effects on the Properties of PET Bottles of Changes to Bottle-Base Geometry

B. Demirel, F. Daver

School of Aerospace Mechanical and Manufacturing Eng., RMIT University, Victoria 3083, Bundoora, Australia

Received 5 January 2009; accepted 23 June 2009
DOI 10.1002/app.30990
Published online 17 August 2009 in Wiley InterScience (www.interscience.wiley.com).

ABSTRACT: Poly(ethylene terephthalate) (PET) bottles are commonly used for packaging of carbonated beverages. Stress cracking in the petaloid-shaped base of the filled bottle has been costly to the beverage industry. This study compares the performance of a standard bottle and a bottle with a base geometry optimized against environmental stress cracking (ESC). The crystallinity of the bottle base is evaluated across the base diameter for both bottles. Moreover, to explain the mechanism of the crack formation and propagation, the cracks in the bottle base are investigated through environmental scanning electron microscopy (ESEM) and optical microscopy. Top-load strength, burst strength, and thermal stability are also reported. © 2009 Wiley Periodicals, Inc. J Appl Polym Sci 114: 3811–3818, 2009

Key words: environmental stress cracking (ESC); poly (ethylene terephthalate) (PET) bottles

INTRODUCTION

Poly(ethylene terephthalate) (PET) is a versatile and commercially important polymer. It has become the material of choice for beverage containers, most commonly for carbonated soft drink (CSD), because it offers excellent clarity, good mechanical and barrier properties, and ease of processing.[1] However, occasional cracking in the petaloid base presents a major inconvenience for the CSD manufacturers and distributors.

Environmental stress cracking (ESC) occurs when the glassy polymer is exposed to an aggressive medium and loaded at low stress for long periods of time.[2–4] Because at least 15% of all plastics failures in service are caused by ESC,[3] investigation of the phenomena is very important for the applications of all engineering plastics.

Although the petaloid shape of the base makes the bottle free-standing (obviating the need for a two-piece bottle), in CSD bottles it increases susceptibility to ESC. Among other factors, material, process conditions and container design have been studied to understand the problem. Crystallinity of the polymer is one of the factors known to be influenced by the process conditions. While some researchers claim that the ESC is due to increased crystallinity[5,6] others claim that crystallinity improves resistance to ESC.[7] It is argued that the overall behavior depends on the polymer, the orientation of the polymer chains inside the polymer matrix, the nature of the ESC agent, and on the way test is carried out; in certain cases the crystallinity may increase or drastically decrease environmental stress-crack resistance (ESCR).[8] The packing pressure during injection molding of the bottle preform[9,10] and the temperature distribution of the preform during stretch blow molding[11] are also known to affect ESC. Hanley et al.[12] have studied the molecular morphology of the petaloid base of PET bottles using small-angle x-ray scattering (SAXS). They reported that the likelihood of failure by cracking is directly related to the morphology in the base. They found that the polymer chains in the central region of the bottle base are circumferentially aligned but non-crystalline, and assumed that the alignment happens during the stretch blow molding stage, whilst the morphology is fixed by quenching the bottles before the chains have time to relax.

So far, only a few simulation studies have been carried out to optimize both the bottle design and the injection stretch blow molding (ISBM) process parameters against ESC. Lyu and Pae reported increased crack resistance in CSD bottles in which the petaloid base was redesigned to minimize the maximum principal stress.[13]

In a previous publication, we demonstrated an optimization methodology combining numerical simulation and a statistical design of experiments approach to optimize the dimensions and geometry of the standard PET bottle base, which reduced the magnitude of the internal stresses resulting from the pressure of carbonated soft drink, thus increasing resistance to environmental stress cracking.[14] In this

Correspondence to: F. Daver (fugen.daver@rmit.edu.au).

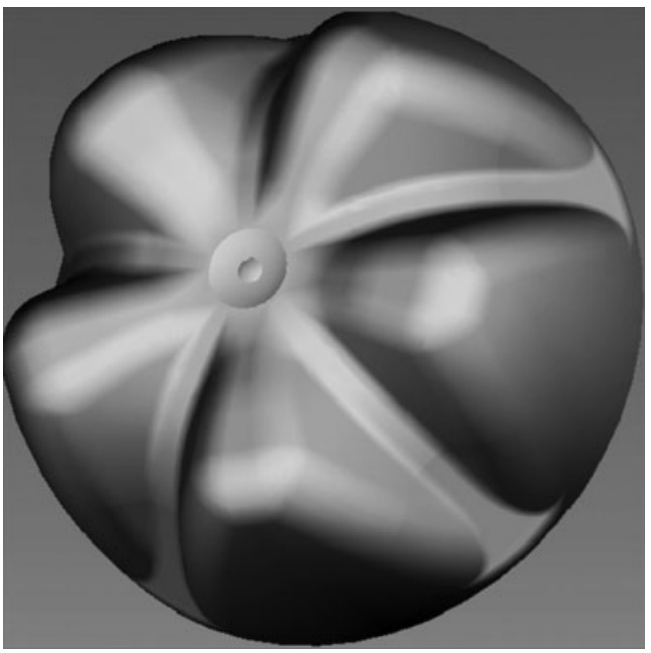

Figure 1 Standard bottle base.

article, we compare the physical and mechanical properties of the new bottle with the current industry standard bottle. The bottles are produced under the same processing conditions and tested for ESCR, top-load strength, burst strength, and thermal stability. The crystallinity of both bottle bases is evaluated using modulated differential scanning calorimeter (MDSC); and the images of the cracks observed in each bottle are obtained through environmental scanning electron microscopy (ESEM) and optical microscope. The mechanism of crack formation and propagation in each bottle base is also compared. The research undertaken aims to verify the optimization results obtained in our previous study[14] by comparing the optimized bottle base with that of standard bottle base and also to bring an understanding of the ESCR mechanism in plastics products in general.

EXPERIMENTAL

Material specification

A PET copolymer (Eastman 9921W) manufactured by Eastman Chemical Company, USA, is used. The polymer is characterized by an intrinsic viscosity of (IV) of 0.80 dL/g; a weight average molecular weight (M_w) of 52,000 g/mol and a number average molecular weight (M_n) of 26,000 g/mol. It has a melt density of 1.2 g/cm^3.

Product and processing conditions

The 1.5-L CSD bottle is produced from a 40 g preform by means of injection stretch blow molding (ISBM). The computer aided design (CAD) images of the standard and optimized bottle bases produced under these process conditions are given in Figures 1 and 2, respectively. The bottle comprises a top section, a rounded base, and a cylindrical midsection. The base comprises five triangular feet configured so that the outer ends are ranged about the outer periphery of the base; the "toes" contact the surface on which the container stands. The central region of the base is cup shaped. The vertical distance between the center base and the plane of outer toes is the base "clearance." Both the standard and the optimized bottles have the same volume and the geometry except the dimensions of the petaloid base motif defined by foot length, valley width, and clearance. The initial values of the standard bottle base parameters are 20 mm, 4.25 mm, 5 mm for the foot length, valley width and clearance, respectively. After an optimization methodology that combines numerical simulation with a statistical design of experiments approach, the foot length, valley width, and clearance parameters of the bottle base are optimized at 29, 8.40, and 5.8 mm, respectively. The ISBM process operating conditions are given in Table I.

Top-load strength

Top-load strength assesses the overall durability of the bottles necessary for filling and stacking the bottles during manufacturing, storage, and distribution. Strength tests are conducted using the INSTRON 4466 instrument equipped with a top-load test

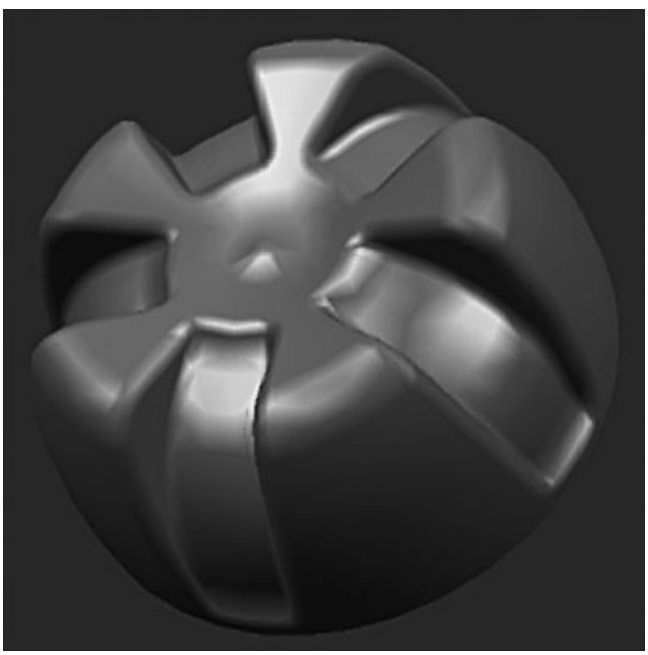

Figure 2 Optimized bottle base.

TABLE I
Injection Stretch Blow Molding Process Parameters for the 1.5 L Bottle Production

Process parameters	
Screw	
Diameter (mm)	38
Screw speed (rpm)	100
Nozzle diameter (mm)	3
Hot runner block (°C)	
Sprue	275
Block	275
Nozzle	295
Barrel temperature (°C)	
Front	275
Middle	275
Rear	270
Nozzle	275
Injection pressure	
Primary (Kgf/cm^2)	140
Secondary (Kgf/cm^2)	60
Injection speed (m/s)	200
Stretch blow molding	
Cold preform temperature (°C)	80
Preform reheat temperature (°C)	109
Preblow (MPa)	1.25
Final blow (MPa)	4
Water temperatures (°C)	Base: 12 Shell: 12 Oven: 10
Machine oil temperature (°C)	35
Stretch Rod speed (m/s)	1.0
Stretch rod outside diameter (mm)	14
Process time (s)	2.48

platform. At least five bottles are tested to achieve an average value.

Burst strength

Burst strength, the pressure at which the bottle bursts, provides an assessment of the overall stability of the bottle under carbonation pressure of the content. It is particularly important in bottles intended for carbonated beverages, to ensure bottles do not blow up at the filling stage and filled bottles do not expand excessively during storage and/or during bottle warming. An AGR plastic pressure tester, with ramp fill capability, is used. At least five bottles are tested to achieve an average value.

Material distribution

To measure the material distribution in the bottle, the bottles are cut into three sections (base, middle, and top) using a hot-wire cutter, custom designed to avoid material loss. The parts of the bottle are separately weighted on a precision scale and recorded for assessment.

Environmental stress-crack resistance

Accelerated stress-crack test unit (ASCRU) and 0.20% sodium hydroxide solution (NaOH) are used for this test. The information about the test unit is of proprietary nature; however, the standard test method information can be obtained from ASTM D 2561 "Standard Test Method for Environmental Stress-Crack Resistance of Blow-Molded Containers."

Thermal stability

The thermal stability test is designed to measure dimensional changes in the bottle as a result of temperature and pressure changes. Satisfactory thermal stability performance is considered to be a critical requirement by the packaging industry. A carbonated product exerts pressure on the inside of the bottle, and this pressure increases with temperature. The pressurized bottle may creep, causing the beverage fill-level to drop.

In thermal stability tests, base clearance, bottle height fill-point drop, and body diameter are recorded for both standard and optimized bottles. Growth in body diameter is measured in terms of changes in the upper, middle, and base section of the bottles. Citric acid, sodium hydrogen carbonate, and sodium carbonate[15] are used to simulate carbonation pressure of the bottle content. The bottles are heated to 38 ± 1°C and stored for 24 h. The parameters mentioned earlier are remeasured at the temperature of 22°C ± 1°C and compared with the precarbonation values.

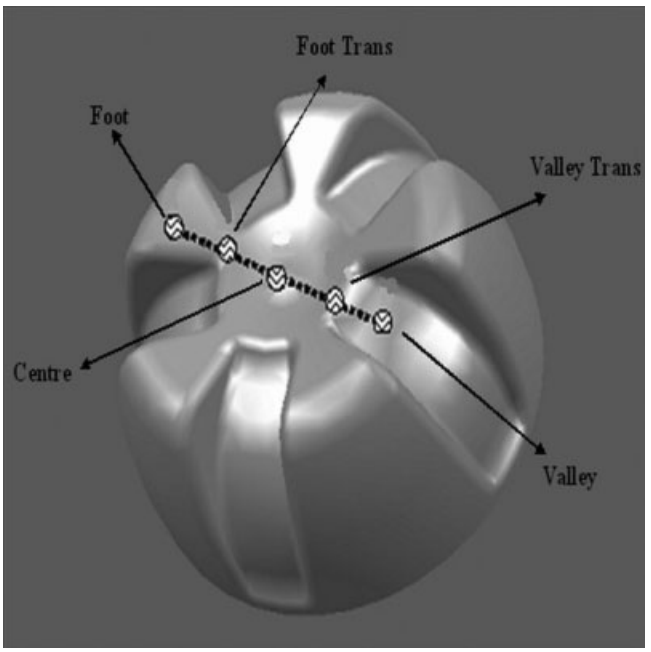

Figure 3 Points for which crystallinity values were calculated by MDSC.

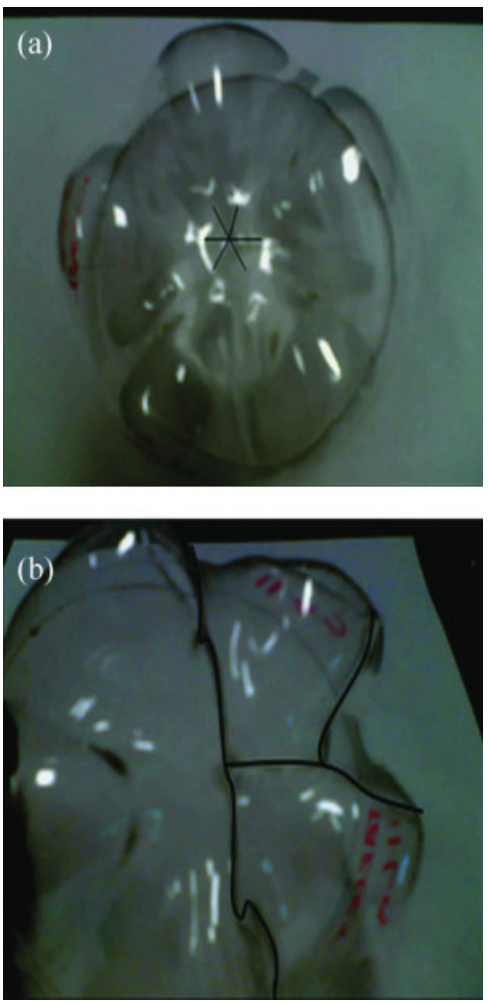

Figure 4 ESC at the bottom of the bottle with standard base (a) central cracks (b) diagonal cracks. [Color figure can be viewed in the online issue, which is available at www.interscience.wiley.com.]

Modulated differential scanning calorimeter

To investigate the reasons for cracking in the bottle base and to explain differences in the ESCR values, crystallinities of both the standard and optimum bottle bases are assessed using MDSC; an MDSC 2920-TA instrument is used for this analysis. Samples of approximately 8–10 mg are crimped in aluminum pans and are scanned at a heating rate of 2°C/min with temperature modulation of ±0.5°C for every 40 s, in a dry nitrogen atmosphere. The degree of crystallinity is determined using eq. (1) considering the heat of fusion of 100% crystalline PET (ΔH_f^o) to be 135 J/g.[16]

$$\chi\ (\%) = \frac{(\Delta H_m - \Delta H_c)}{\Delta H_f^o} \qquad (1)$$

Where ΔH_m and ΔH_c are the enthalpy of melting and the enthalpy of crystallization, respectively.

Figure 5 ESC at the bottom of the bottle with optimum base. [Color figure can be viewed in the online issue, which is available at www.interscience.wiley.com.]

In this study, the percentage crystallinity in the bottle base is assessed at five critical points across the base diameter as shown in Figure 3.

Environmental scanning electron microscopy (ESEM) and optical microscopy

To understand and identify the mechanism of the crack formation and propagation, cracks in both standard and optimized bottles are studied through environmental scanning electron microscopy (FEI Quanta 200 ESEM) and optical microscopy (Olympus Twin Optic Microscope). Specimens used in the analysis are collected from the ESCR test samples.

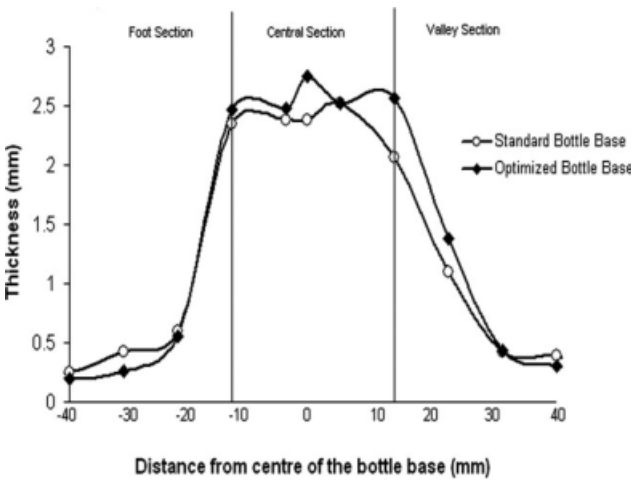

Figure 6 Thickness of the bottles with standard and optimized base.

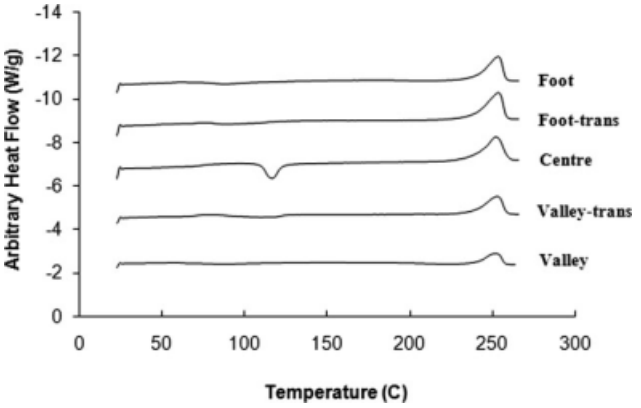

Figure 7 MDSC diagrams of the standard bottle base.

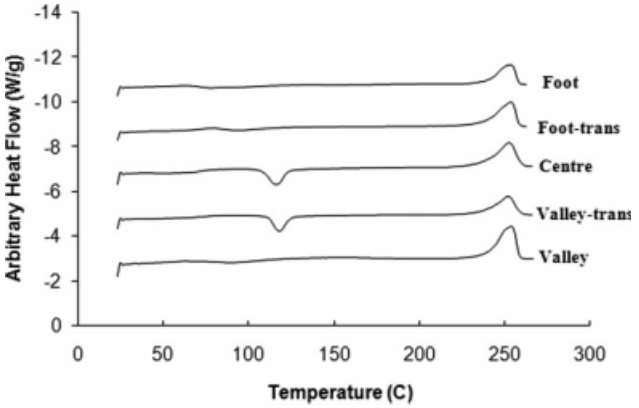

Figure 8 MDSC diagrams of the optimized bottle base.

This test method has been useful in explaining the initial crack location, its direction, and the differences in resistance to cracking.

Simulation of internal stress in the bottle base under ESCR test conditions

Stress in the bottle base arising from the carbonation pressure of the content is simulated through finite-element models of each bottle design, under conditions similar to the accelerated environmental stress cracking test conditions. FE models of the bottles are developed via CATIA. Simulated stress and the actual thickness variations across the bottle base are compared for both bottles.

EXPERIMENTAL RESULTS AND DISCUSSION

Burst strength

Burst strength indicates the maximum pressure that the bottle can bear at the time of failure. The burst strength is found to be 14.1 and 13.4 bar for the standard and the optimized bottles, respectively. Both bottles fulfill the commercial minimum burst strength requirement of 7 bar for CSD applications. Similarly, the volumetric expansions of the bottles, 579 and 541 mL for the standard and the optimized bottles, respectively, are within the limit required by the industry.

Top-load strength

The top-load strength is found to be 31.1 and 29.2 kg for the standard and the optimized bottles, respectively. Both values are adequate for CSD packaging applications.[15]

Environmental stress cracking resistance

Stress-crack resistance is much higher in the optimized bottle base. The ESCR time is 64 ± 18 minutes for the optimized bottles compared with only 34 ± 10 min for the standard bottles.

Figures 4 and 5 show the cracks in the standard and redesigned bases, respectively. In the standard base, the cracks developed both radially in the center of the base [Fig. 4(a)] and diagonally across the base [Fig. 4(b)]. However, in both base designs, the cracks develop mainly in the center of the base. This is explained due to the abrupt changes in thickness in this region (Fig. 6) compared with gradual changes in the foot and valley regions. In addition, it is found that the thickness in the valley region is higher than the foot region for both bottle bases.

TABLE II
Properties of the Selected Points in the Standard Bottle Base

	1st heating					Cooling		2nd heating				χ
Location on the base	T_g (°C)	T_{cc} (°C)	ΔH_{cc} J/g	T_m (°C)	ΔH_m (J/g)	T_c (°C)	ΔH_c J/g	T_g (°C)	T_{m1} (°C)	T_{m2} (°C)	ΔH_m (J/g)	(%)
Foot	78.4	89.5	5.5	253.6	45.3	201.2	39.8	81.0	242.4	252.7	37.4	43.4
Foot trans	70.9	90.6	5.9	253.7	43.2	198.9	37.1	79.6	242.3	252.0	35.8	32.2
Centre	73.2	116.8	15.9	252.3	41.7	198.3	37.7	81.7	241.7	252.3	39.2	10.0
Valley trans	78.4	110.3	9.4	253.0	39.9	198.9	33.4	81.6	241.8	252.0	34.5	23.0
Valley	75.0	88.1	5.9	252.9	44.1	199.4	39.2	79.7	240.6	251.9	37.8	51.8

TABLE III
Properties of the Selected Points in the Optimum Bottle Base

Location on the base	1st heating					Cooling		2nd heating				χ
	T_g (°C)	T_{cc} (°C)	ΔH_c J/g	T_m (°C)	ΔH_m (J/g)	T_c (°C)	ΔH_c J/g	T_g (°C)	T_{m1} (°C)	T_{m2} (°C)	ΔH_m (J/g)	(%)
Foot	79.1	77.8	12.8	253.4	45.2	202.5	40.1	78.7	242.9	251.7	36.0	31.2
Foot trans	75.7	95.9	6.3	253.5	43.3	202.4	35.5	82.1	243.3	252.3	35.9	38.2
Centre	76.5	116.0	18.2	252.4	39.5	201.7	36.9	82.2	243.1	252.3	37.1	14.1
Valley trans	72.3	114.5	20.1	252.3	41.1	202.8	41.8	80.4	243.7	252.0	38.6	14.4
Valley	78.6	91.2	5.0	253.9	46.3	202.7	41.6	81.8	243.0	252.3	38.5	50.3

Thermal stability

Thermal stability tests measured percentage changes in base clearance, bottle height, fill-point drop, and body diameter. According to industry practice, the optimized bottle provided adequate thermal stability.

Clearance height in the standard base is changed from 7.2 to 2.8 mm and from 6.2 mm to 1.7 mm in the optimized base. However, the percentage change is similar for both bottles. The fill-point drop, which is the change in the beverage level in the bottle, is 1.1 mm less for the optimized bottle: 21.8 mm compared with 22.9 mm.

Growth in the bottle body is found to be similar for both standard and optimized bottles. For the standard bottle, the changes the upper, middle, and the base section diameters are 2.2, 2.4, and 1.4 mm, respectively. The corresponding changes for the optimized bottle are 2.4, 2.3, and 1.6 mm.

Crystallinity

By means of the MDSC method, the crystallinity values at critical points in the bottle base are calculated. Figures 7 and 8 show the heat flow curves for the standard base and the optimized base, respectively. From these curves, thermal characteristics such as glass transition temperature (T_g), cold crystallization temperature (T_{cc}), crystallization temperatures (T_c), and melting point (T_m) are obtained, along with percent crystallinity (% χ).

Tables II and III give the thermal characterization parameters and percentage crystallinities for the standard optimized bases, respectively. Glass transition temperatures (T_g), which are related to amorphous structure of the material, vary between 6°C and 8°C for standard and optimized bottle base, respectively; it is not possible to observe any trend. Although the crystallization temperatures (T_c) are found to be slightly higher for the optimized bottle base, crystallization temperatures (T_c) do not demonstrate a particular trend in either bottle base. Cold crystallization temperature (T_{cc}) for both bottles shows an increase in the base center. This is also

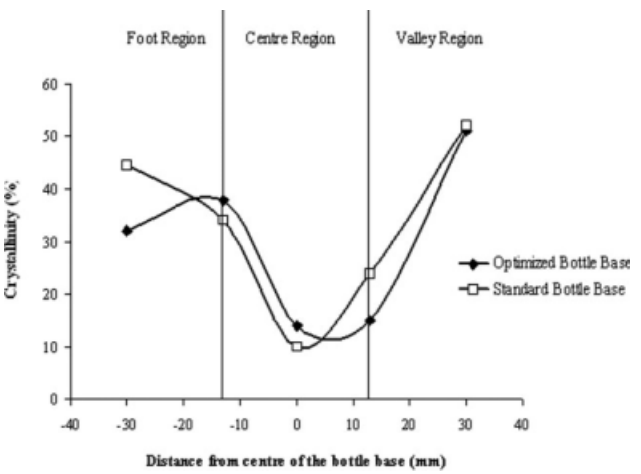

Figure 9 Actual crystallinity in the optimum and standard bottle bases.

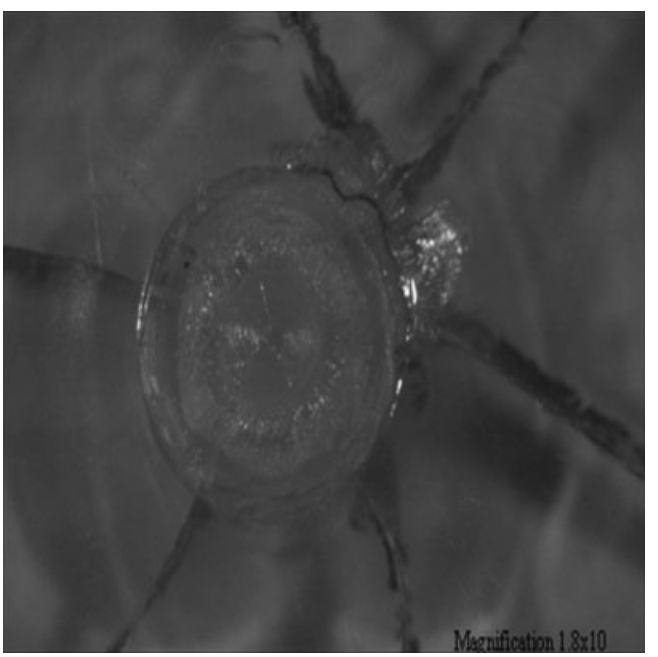

Figure 10 Optical microscope images of the cracks around the center of optimum base.

reflected in low cystallinity of 10–14% in these regions.

Crystallinity values decrease toward the center of the base for both bottles as shown in Figure 9. The crystallinity of the optimized base is higher (38.2%) than the standard base (32.2%) for the foot transition region, i.e., between the center and the foot. However, the result is reversed for the valley transition region, i.e., between the center and the valley; the crystallinity of the optimized base is lower than the standard base; 14.4% compared with 23.0%. In the valley region, the crystallinity values are similar for both base designs: 50.3% and 51.8%. However, in the central region, where environmental stress cracking is mainly observed, crystallinity in the optimized base (14%) is higher than in the standard base (10%).

Crack formation and propagation

In both bottle designs, cracks in the bottle base are initiated at the injection pin, which acts a stress concentration point. As shown in the optical microscopy image of the bottle base (Fig. 10), cracks do not exactly pass through the base center. In the optimized base, the cracks are contained within the central region and do not reach the foot or the valley of the base. In the standard base, however, in some samples, diagonal cracks appear across the transition regions in addition to the central cracks.

There are clear differences between the appearance of cracks found in the standard and the new bottle base. The cracks in the standard bottle base propagate in a rather straight manner (Fig. 11),

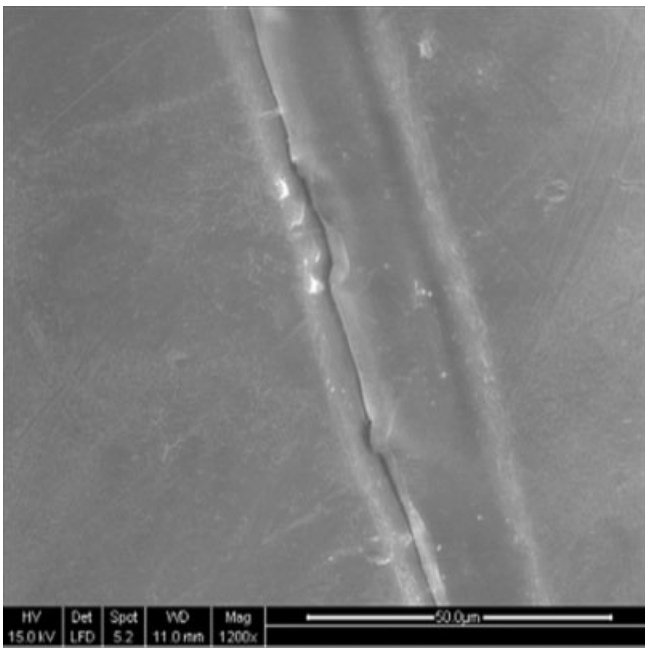

Figure 11 SEM image of the crack propagation in the standard bottle base.

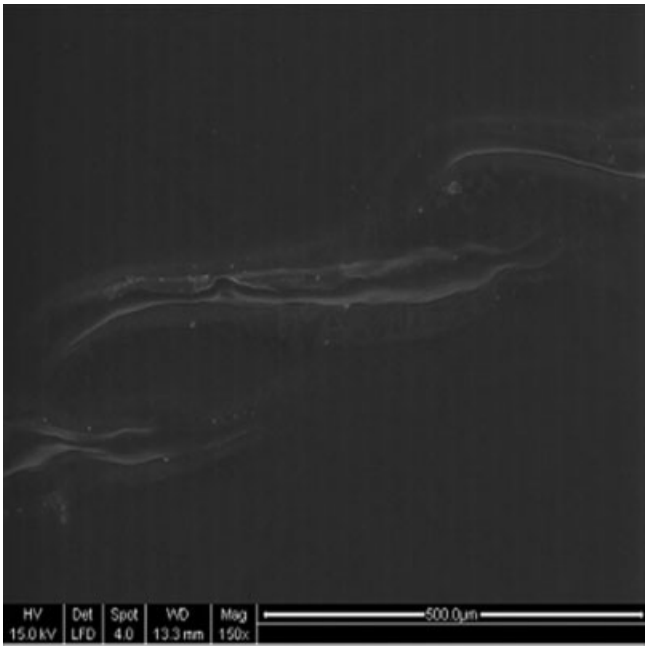

Figure 12 SEM image of the crack propagation in the optimized model.

whereas for the optimized bottle base, cracks take up a spiral form, demonstrating a fibrous appearance (Fig. 12). Despite the fact that both bottles are produced under the same standard process operating conditions and made out of the same material, the mechanisms of crack formation and propagation appear to be significantly different, resulting in significant differences in ESCR times.

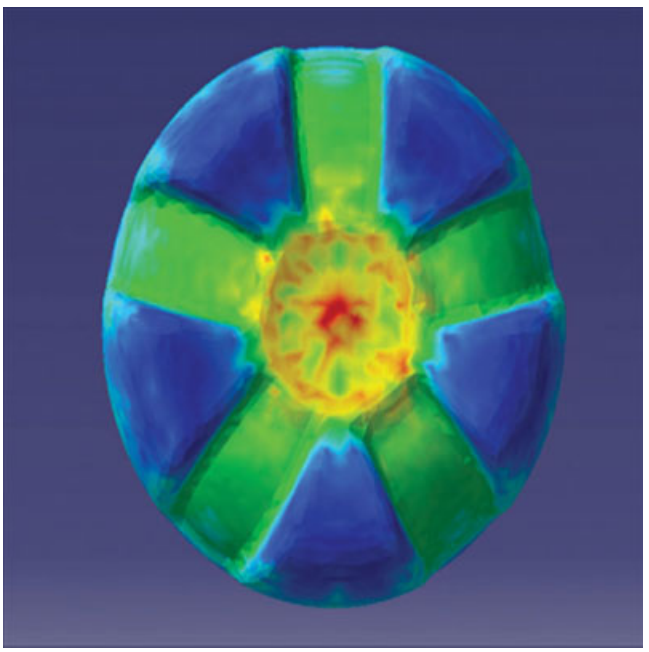

Figure 13 Simulation of the stress in the optimized bottle base under load. [Color figure can be viewed in the online issue, which is available at www.interscience.wiley.com.]

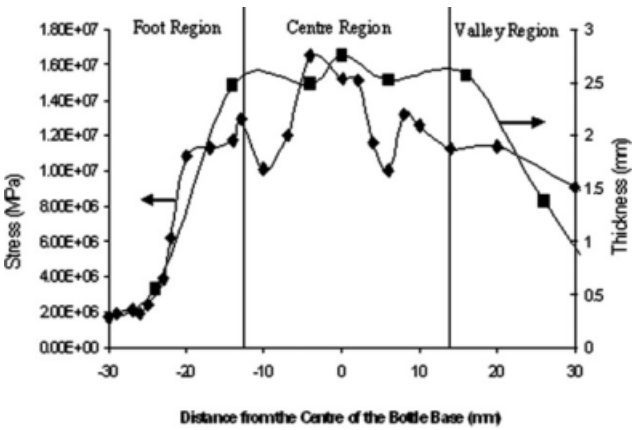

Figure 14 Simulated stress and measured thickness in the optimized bottle base.

Relationship of ESCR to that of physical and mechanical properties of the bottle base

Cracks occur within the central zone of the optimized base design. In this region, the crystallinity values are lower than other regions of the base. In the CATIA stress simulation studies, conducted under the stresses similar to accelerated environmental stress cracking test conditions, the highest stress values are also found to occur in the center region of the base. For the optimized and standard bottles bases, the bottle base thickness and the simulated stress values are shown in Figures 13 and 14, respectively. Simulated stress for the standard bottles is approximately 7 MPa higher compared with the optimized bottles within the center zone of the bottles (10 mm from the bottle center) with a corresponding decrease of 6 mm in the base thickness. This reinforces our hypothesis that the increase in ESCR is most likely attributable the modified base geometry reducing the stress generated by the carbonation pressure stress.

CONCLUSION

In this article, the physical, mechanical, and geometrical changes in the PET bottle resulting from a redesigned petaloid base are assessed by the appropriate test methods. The optimization study has been effective and has led to significantly increased ESCR. Changes to the base geometry have slightly increased the amount of material transferred from the body to the base, hence the equivalent stress in the base is reduced at this modified geometry. The increased ESC resistance of the modified base can be explained by the fact that the changes to the base geometry reduce the internal stress inside the bottle, along with a slight increase in the base thickness.

It is concluded that the geometrical modification of the standard bottle base reduces the magnitude of the internal stress resulting from the carbonation pressure of the content. Hence, the optimized bottle, exposed to environmental stress cracking agents, shows improved crack resistance without jeopardizing other relevant properties of the bottles.

The authors thank Prof. Dougal McCulloch and Dr. Philip Francis (Applied Sciences—Science, Engineering and Technology Portfolio) for providing access to the environmental scanning electron microscopy (ESEM) in the RMIT microscopy and microanalysis facility, and Mr. Peter Cooper for his guidance during ESEM and optical microscopy studies.

References

1. Martin, L.; Stracovsky, D.; Laroche, D.; Bardetti, A.; Ben-Yedder, R.; Diraddo, R. Soc Plast Eng Annu Tech Conf Tech Pap 1999, 1, 982.
2. Rosato, D. V. Blow Molding Handbook; Oxford University Press: Oxford, 1989.
3. Wright, D. Environmental Stress Cracking of Plastics; Rapra Tech Ltd: Shawbury, 1996.
4. Howard, J. B. J Soc Plast Eng 1959, 15, 397.
5. Soares, J. B. P.; Abbott, R. F.; Kim, J. D. J Polym Sci 2000, 38, 1267.
6. Jabarin, S. A.; Lofgren, E. A. Polym Eng Sci Polym Phys Ed 1992, 32, 146.
7. Abu-Isa, I. A.; Jaynes, C. B.; O'Gara, J. F. J Appl Polym Sci 1996, 59, 1958.
8. Sanches, N.deB.; Dias, M. L.; Pacheco, E. B. A. V. Polym Eng Sci 2008, 48, 1953.
9. Brooks, D. W.; Giles, G. A. PET Packaging Technology; Academic Press: Sheffield, 2002.
10. Zagarola, S. W. Soc Plast Eng Annu Tech Pap 2000, 1, 895.
11. Venkateswaran, G.; Cameron, M. R.; Jabarin, S. A. Adv Polym Tech 1998, 17, 237.
12. Hanley, T.; Sutton, D.; Cookson, D.; Koisor, E.; Knott, R. J Polym Sci 2006, 99, 3328.
13. Lyu, M. Y.; Pae, Y. J Appl Polym Sci 2003, 88, 1145.
14. Demirel, B.; Daver, F. J Appl Polym Sci 2009, 114, 1126.
15. Chemical Carbonation Reference Technical Manual 3–1, Pepsi-Cola Company, North America. PET Package Specifications and Qualification Manual, Issue Date 11/96. An internal Pepsi-Cola Company Report; p 44.
16. Mehta, A.; Gaur, U.; Wunderlich, B. J Polym Sci Polym Phys Ed 1978, 16, 289.